

# Development of a New Brushless Doubly Fed Doubly Salient Machine for Wind Power Generation

Ying Fan<sup>1,2</sup>, K. T. Chau<sup>1</sup>, and Shuangxia Niu<sup>1</sup>

<sup>1</sup>Department of Electrical and Electronic Engineering, University of Hong Kong, Hong Kong, China

<sup>2</sup>Department of Electrical Engineering, Southeast University, Nanjing 210096, China

This paper proposes and implements a new three-phase 12/8-pole brushless doubly fed doubly salient machine (BDFDS) for wind power generation. The key is to design and control the proposed BDFDS machine in such a way that the system can offer constant output voltage and efficiency optimization over a wide range of wind speeds. First, the machine output power equation is derived to initialize the machine dimensions. Second, finite-element analysis is performed to finalize the machine dimensions as well as to determine the machine parameters and characteristics. Third, the system model is formulated and applied for computer simulation. Finally, the whole system is prototyped for verification, with emphasis on the constant voltage regulation and efficiency optimization.

**Index Terms**—Brushless, doubly fed, doubly salient, wind power generation.

## I. INTRODUCTION

WITH ever increasing concerns on energy crisis and environmental protection, the development of renewable energy resources has taken on an accelerated pace. Wind power is one of the most viable renewable energy resources, and its core element is the electric machine—the generator.

Conventional generators, such as the synchronous and induction ones, are mainly designed for constant-speed wind power operation. Since they are connected across the grid, their speed is mainly limited by the frequency of the grid. With the maturity of power electronics, various machines can be utilized for variable-speed wind power generation. In [1], the doubly salient permanent magnet (DSPM) machine, incorporating the structure of a switched reluctance (SR) machine and the use of PM material, was proposed for wind power generation. Although this DSPM generator offers the advantages of high power density and high robustness, it suffers from the drawbacks of high PM cost and uncontrollable flux. In [2], with the replacement of PMs in the DSPM motor by a dc field winding, the (BDFDS) motor was proposed for electric vehicles (EVs). By using dc field current control, this motor offers the definite advantage that it can provide wide-range constant-power operation for EV cruising at which the input voltage is fixed at the rated value. The purpose of this paper is to reverse and further extend this idea. Namely, with the use of dc field current control, the BDFDS generator can provide constant output voltage and efficiency optimization for a wide range of wind speeds.

It should be noted that those available wind power generators, including the synchronous and induction ones, are incapable of offering constant voltage regulation or efficiency optimization, which are highly desirable.

## II. DESIGN AND ANALYSIS

Fig. 1 shows the configuration of the proposed BDFDS machine system for wind power generation. It mainly consists of a

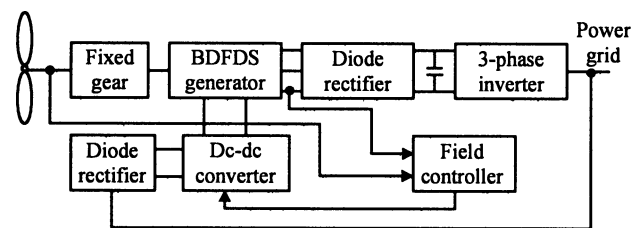


Fig. 1. System configuration.

wind turbine for capturing wind power, a fixed gear to step up the wind speed for high-speed operation, a three-phase BDFDS generator for the desired electromechanical energy conversion, two diode rectifiers for ac-dc conversion, a three-phase six-step inverter for dc-ac conversion with minimum switching loss, as well as a dc-dc converter and a field controller for machine field regulation.

First of all, the rated speed of the proposed BDFDS machine needs to be identified since it affects the sizing of the whole system. For a horizontal axis wind turbine, the mechanical output power  $P_{\text{mech}}$  is typically expressed as [3]

$$P_{\text{mech}} = \frac{1}{2} C_p \rho v_w^3 A \quad (1)$$

where  $C_p$  is the coefficient of wind power,  $\rho$  is the air density,  $v_w$  is the wind speed, and  $A$  is the swept area of wind turbine rotor. Normally, a wind turbine is rated at a wind speed of 12.5 m/s. So, by selecting the gearbox ratio as 1 : 5.7, the rated speed of the BDFDS generator is 1500 rpm.

Fig. 2 shows the proposed three-phase 12/8-pole (12 stator poles and eight rotor poles) BDFDS machine. It adopts the same structure as an SR machine, namely saliency on both the stator and rotor. There are no windings or PMs on the rotor, whereas there are two types of windings on the stator—a polyphase armature winding and a dc field winding. Since the dc current flowing through the field winding can be independently controlled, this arrangement can solve the problem of uncontrollable PM flux.

Similar to the derivation for a DSPM machine [4], the output power  $P_2$  of the BDFDS machine can be derived as

$$P_2 = \frac{0.87\pi^2}{120} \frac{N_r}{N_s} k_d k_e k_i A_s B_\delta n_s \eta D_{is}^2 l_{ef} \quad (2)$$

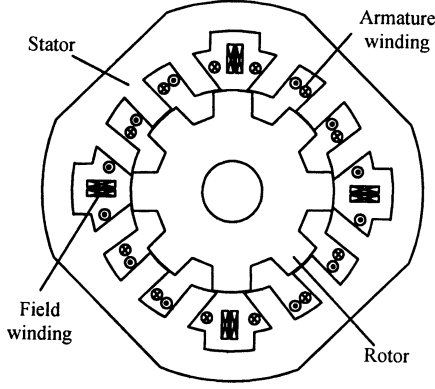


Fig. 2. Proposed three-phase 12/8-pole BDFDS machine.

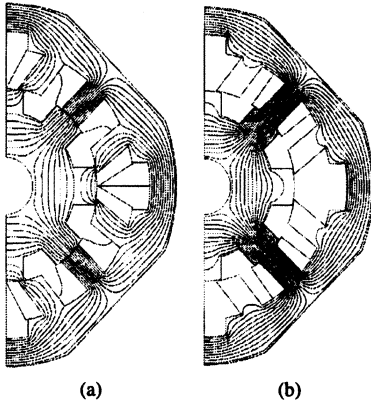


Fig. 3. Magnetic field distributions. (a) Field current only. (b) Armature current only.

where  $N_s$  and  $N_r$  are the stator and rotor pole numbers, respectively,  $k_d$  the flux leakage factor,  $k_e$  the ratio of terminal voltage to no-load EMF,  $k_i$  the ratio of current amplitude to RMS current,  $A_s$  the electric loading of stator,  $B_\delta$  the airgap flux density,  $n_s$  the rated speed,  $\eta$  the machine efficiency,  $D_{is}$  the inner diameter of the stator, and  $l_{ef}$  the effective stack length.

In accordance with the basic operating principle of the BDFDS machine, the relationship between the number of stator poles and the number of rotor poles is given by

$$N_s = 2mk \quad N_r = N_s \pm 2k \quad (3)$$

where  $m$  is the number of phases, and  $k$  is a positive integer. Also, the number of rotor poles is usually less than that of stator poles so as to facilitate commutation, and the number of phases should be equal to or greater than 3 so as to allow for self-starting. For three-phase operation, the 6/4-pole and 12/8-pole configurations are possible choices. As compared to the 6/4-pole one, the 12/8-pole machine possesses shorter flux paths in yoke, hence resulting in lower iron loss. Also, the 12/8-pole one offers halved flux per pole and hence halved width of stator teeth, leading to shorter end windings and hence lower copper loss. Therefore, the 12/8-pole configuration is selected.

By using the finite-element analysis (FEA), the static characteristics of the BDFDS machine are deduced. Fig. 3 shows the magnetic field distributions due to the field current only and the armature current only, respectively. Based on these distributions, the machine dimensions and parameters can be fine

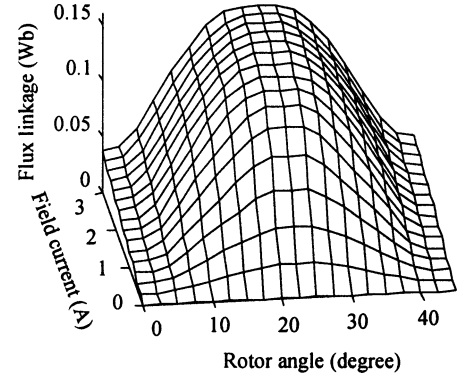


Fig. 4. Flux linkage characteristics.

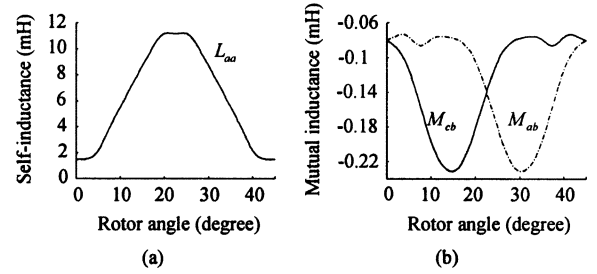


Fig. 5. Inductance characteristics. (a) Self. (b) Mutual.

tuned. Moreover, the machine characteristics, including the flux linkage, self-inductance, mutual inductance, and no-load EMF, can be obtained. The corresponding flux linkage which varies with both the rotor angle and field current is shown in Fig. 4. The characteristics of self-inductance and mutual inductances are also shown in Fig. 5.

### III. MODELING AND CONTROL

Based on the parameters obtained from the FEA, the model of the BDFDS machine can be formulated as

$$\frac{d}{dt} \begin{pmatrix} L_{aa} & M_{ab} & M_{ac} & M_{af} \\ M_{ba} & L_{bb} & M_{bc} & M_{bf} \\ M_{ca} & M_{cb} & L_{cc} & M_{cf} \\ M_{fa} & M_{fb} & M_{fc} & L_{ff} \end{pmatrix} \begin{bmatrix} i_a \\ i_b \\ i_c \\ i_f \end{bmatrix} = \begin{bmatrix} v_a \\ v_b \\ v_c \\ v_f \end{bmatrix} + \begin{bmatrix} R_a & 0 & 0 & 0 \\ 0 & R_b & 0 & 0 \\ 0 & 0 & R_c & 0 \\ 0 & 0 & 0 & R_f \end{bmatrix} \begin{bmatrix} i_a \\ i_b \\ i_c \\ i_f \end{bmatrix} \quad (4)$$

where  $L_{aa}, L_{bb}, L_{cc}$  are the phase self-inductances,  $L_{ff}$  is the field self-inductance,  $M_{ab}, M_{bc}, \dots, M_{fc}$  are the mutual inductances,  $i_a, i_b, i_c$  are the phase currents,  $i_f$  is the field current,  $v_a, v_b, v_c$  are the phase voltages,  $v_f$  is the field voltage,  $R_a, R_b, R_c$  are the armature winding resistances, and  $R_f$  is the field winding resistance.

With the use of this machine model, system control can be performed. As shown in Fig. 1, the core of system control is the field controller. On one hand, it measures the input wind speed and hence deduces the mechanical power using (1). On the other hand, it measures the generated output voltage and power of the BDFDS machine. Consequently, this controller performs two tasks. First, when the generated output voltage deviates from the preset value due to the variation of wind speeds, the field

TABLE I  
SPECIFICATION OF PROPOSED BDFDS MACHINE

Rated speed	1500 rpm
Rated power	750 W
Stator inner diameter	75 mm
Stator outer diameter	140 mm
Stack length	75 mm
Air-gap length	0.30 mm
Stator pole arc	15°
Rotor pole arc	22°

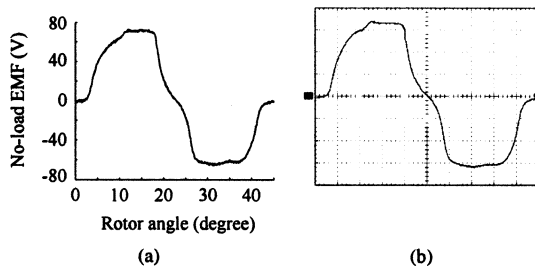


Fig. 6. No-load EMF waveforms. (a) Simulated. (b) Measured (20 V/div, 500  $\mu$ s/div).

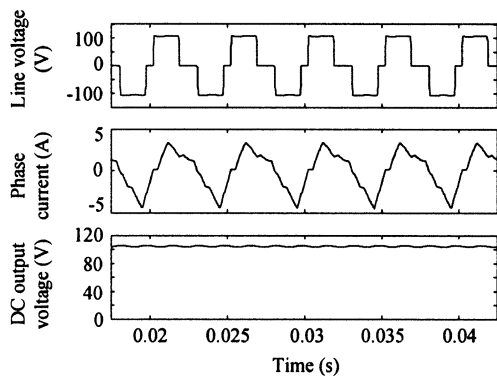


Fig. 7. Simulated waveforms of line voltage, phase current, and dc output voltage.

controller tunes the dc field current to achieve constant output voltage. Second, based on the measured mechanical input power and electrical output power, the dc field current is fine tuned to maximize the system efficiency.

#### IV. SIMULATION AND EXPERIMENTATION

Computer simulation using MATLAB is based on the machine model as given by (4). Experimentation is based on the designed machine with specifications as listed in Table I. The natural wind characteristics are emulated by real-time controlling a programmable dc dynamometer.

Fig. 6 shows the simulated and measured no-load EMF waveforms at the rated speed. As expected, the agreement is very good. Moreover, Fig. 7 shows the simulated waveforms of the machine line voltage and phase current as well as the rectified dc output voltage at the rated conditions with the field current of 1 A, whereas Fig. 8 shows the measured counterparts. It can be found that these operating waveforms are closely matched.

By online tuning the field current, the dc output voltage can be maintained constant over a wide range of rotor speeds or

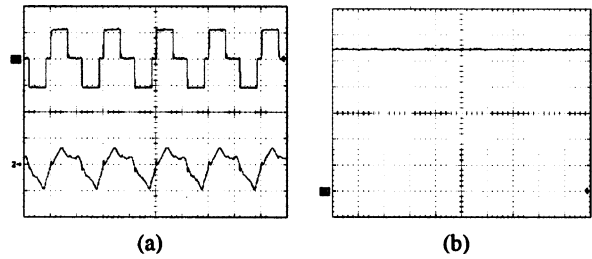


Fig. 8. Measured waveforms. (a) Line voltage and phase current (100 V/div, 5 A/div, 2.5 ms/div). (b) DC output voltage (20 V/div, 2.5 ms/div).

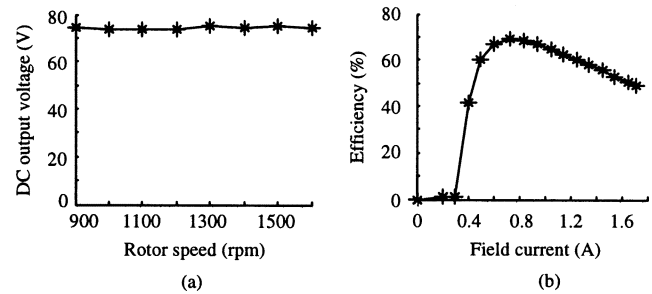


Fig. 9. Measured characteristics. (a) DC output voltage versus speed. (b) Efficiency versus field current.

wind speeds as shown in Fig. 9(a). Also, by fine tuning the field current, the machine efficiency can be optimized as shown in Fig. 9(b). Therefore, it confirms that both the voltage regulation and efficiency optimization can be achieved by tuning the field current of the proposed machine.

#### V. CONCLUSION

In this paper, a new three-phase 12/8-pole BDFDS machine system has been proposed and implemented for wind power generation. Theoretical derivation, electromagnetic field analysis, system modeling, and field current control have been discussed. Both computer simulation and experimental results have been given to verify the validity of the proposed system, particularly the constant voltage regulation and efficiency optimization.

#### ACKNOWLEDGMENT

This work was supported by the Research Grants Council of Hong Kong Special Administrative Region, China, under Project HKU 7111/05E.

#### REFERENCES

- [1] Y. Fan, K. T. Chau, and M. Cheng, "A new three-phase doubly salient permanent magnet machine for wind power generation," *IEEE Trans. Industry Appl.*, vol. 42, pp. 53–60, 2006.
- [2] K. T. Chau, M. Cheng, and C. C. Chan, "Nonlinear magnetic circuit analysis for a novel stator doubly fed doubly salient machine," *IEEE Trans. Magn.*, vol. 38, pp. 2382–2384, 2002.
- [3] J. Chen, C. V. Nayar, and L. Xu, "Design and finite-element analysis of an outer-rotor permanent magnet generator for directly coupled wind turbines," *IEEE Trans. Magn.*, vol. 36, pp. 3802–3809, 2000.
- [4] M. Cheng, K. T. Chau, and C. C. Chan, "Design and analysis of a new doubly salient permanent magnet motor," *IEEE Trans. Magn.*, vol. 37, pp. 3012–3020, 2001.